ACS OMEGA

http://pubs.acs.org/journal/acsodf

Article

Quantitative Assessment Method of Muzzle Smoke in a Field Environment

Chenguang Yan, Chen-guang Zhu,* Mingxing Zhang, and Yan Li*

Cite This: *ACS Omega* 2023, 8, 7950−7955

Read Online

ACCESS | Metrics & More | Article Recommendations

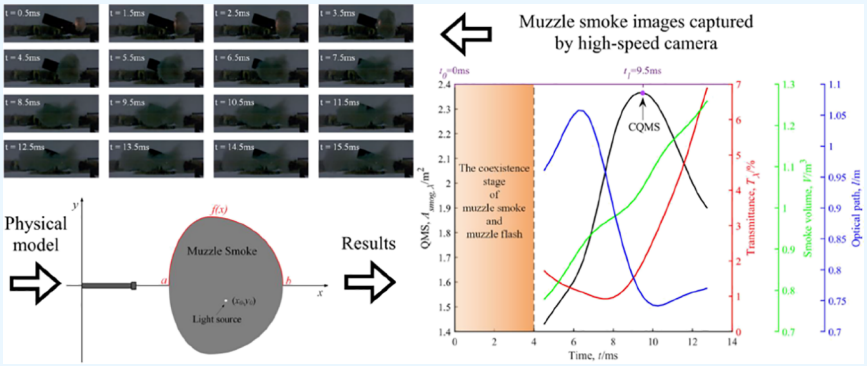

ABSTRACT: The muzzle of barrel weapons produces a large amount of smoke (muzzle smoke), a major source of pollution in the battlefield. Quantitative assessment of muzzle smoke is an important support for the development of advanced propellants. However, due to the lack of effective measurement methods for field experiments, most of the previous studies were based on a smoke box, and few studies have focused on muzzle smoke in the field environment. In view of the nature of the muzzle smoke and the conditions of the field environment, the characteristic quantity of muzzle smoke (CQMS) was defined based on the Beer−Lambert law in this paper. CQMS is used to characterize the danger level of muzzle smoke produced by the propellant charge, and theoretical calculations indicated that when the transmittance is e^{-2}, the impact of the measurement errors on CQMS can be minimized. Seven firings with the same propellant charge of a 30 mm gun were carried out in a field environment to verify the effectivity of CQMS. The measurement uncertainty analysis on the experimental results showed that the CQMS of the propellant charge used in this study was 2.35 ± 0.06 m^2, which indicates that CQMS can be used to quantitatively assess muzzle smoke.

1. INTRODUCTION

A large amount of smoke is usually generated at the muzzle when the barrel weapon based on chemical energy is firing, which will not only hinder their own shooting speed and accuracy[1] but also pose a risk to human health.[2,3] In addition, muzzle smoke can also be detected by an optical detection system[4] (Zhou et al.), thereby exposing the location of the shooter. Researchers engaged in propellant research have always paid attention to this harmful phenomenon and kept seeking technical ways to reduce muzzle smoke.[5−8] In any case, quantitative assessment of muzzle smoke is the key to guaranteeing this research.

According to the classification of the experimental environment, there are usually two methods for muzzle smoke assessment. One method is the smoke-box method, which is suitable for small arms. A measurement method for muzzle smoke was proposed and the results of the experiment were analyzed, providing the foundation for subsequent research.[9] A pressure-removable smoke box was used to measure smoke concentration using dual optical path length measurement.[10] A quantitative detection system was designed to characterize the smoke concentration of the muzzle smoke of small arms, and the system measures the photosensitive voltages of the penetrating laser through the space of the muzzle smoke box in the states with and without smoke.[11] The traditional method was improved to avoid the impact of the residue in the smoke box.[12] In general, researchers only focus on the smoke concentration because the smoke box has a fixed volume and a fixed optical path length. The other method is a field experiment, which is equivalent to the user's actual environment. Steward et al.[13] characterized and discriminated firing signatures of a large caliber gun based on two hundred and one

Received: December 5, 2022
Accepted: February 7, 2023
Published: February 15, 2023

https://doi.org/10.1021/acsomega.2c07764
ACS Omega 2023, 8, 7950−7955

firings of three 152 mm howitzer munitions. Zhao et al.[14] took the integral of absorbance over time as characteristic smoke capacity according to the visible light transmittance of muzzle smoke in an open system.

Different from the smoke-box method, volume and optical path length are not fixed in the field environment, so it is questionable to only focus on the smoke concentration or any other single physical quantity. The purpose of this research is to provide a reliable, reproducible, and easy-to-implement method for identifying the danger level of muzzle smoke in the field environment.

2. MATERIALS AND METHODS

2.1. Definition of CQMS. According to the Beer−Lambert law

$$A = \log\left(\frac{1}{T_\lambda}\right) = \varepsilon_\lambda l c \tag{1}$$

where A is the absorbance; T_λ is the transmittance of the material; ε_λ is the absorptivity of the attenuating species; l is the optical path length; and c is the concentration of the attenuating species, and in this study

$$c = \frac{m}{V} \tag{2}$$

where m is the mass of muzzle smoke; and V is the smoke volume.

The mass of muzzle smoke increases with the discharge of smoke from the barrel in the early stage and decreases with the loss of smoke in the later stage. The moment when the mass of muzzle smoke takes the maximum is represented by t_1. Eq 1 at t_1 can be rewritten as

$$m_{t_1}\varepsilon_\lambda = -\frac{\log(T_{\lambda,t_1})\cdot V_{t_1}}{l_{t_1}} \tag{3}$$

For muzzle smoke produced by the same formulation and batch of propellant charges under the same experimental conditions, maximum mass m_{t_1} and absorptivity ε_λ of muzzle smoke can be regarded as constant values. Namely, the left term of eq 3 is theoretically a constant value. However, it is difficult to obtain the accurate value of m_{t_1} and ε_λ of muzzle smoke through the existing test methods in the field environment. On the contrary, the quantity of the right term of eq 3 can be obtained relatively easily, CQMS (denoted by $A_{\mathrm{smog},\lambda,t_1}$) is defined as

$$A_{\mathrm{smog},\lambda,t_1} = -\frac{\log(T_{\lambda,t_1})\cdot V_{t_1}}{l_{t_1}} \tag{4}$$

Similarly, the quantity of muzzle smoke (QMS, denoted by $A_{\mathrm{smog},\lambda}$) at any time is defined as

$$A_{\mathrm{smog},\lambda} = -\frac{\log(T_\lambda)\cdot V}{l} \tag{5}$$

The muzzle smoke is axisymmetric along the central axis of the barrel, and the light source and the camera were placed on both sides of the muzzle smoke. The schematic diagram of the muzzle smoke taken by the camera is shown in Figure 1. Thus, the smoke volume can be calculated as

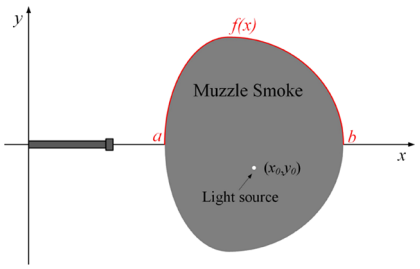

Figure 1. Schematic diagram of the muzzle smoke.

$$V = \pi \int_a^b [f(x)]^2 \mathrm{d}x \tag{6}$$

where a and b are the left and right limits of the muzzle smoke in the x-axis, respectively; $f(x)$ is the function represented by the edge of the smoke on the upper part of the x-axis.

Discretizing eq 6

$$V = \pi l_{\mathrm{pixel}} \sum_{i=a}^{b} [f(x_i)]^2 \tag{7}$$

where l_{pixel} is the actual length of a single pixel of the camera corresponding to the plane in Figure 1.

The optical path length is given by

$$l = 2\sqrt{f(x_0)^2 - y_0^2} \tag{8}$$

where (x_0, y_0) represents the position of the light source in Figure 1.

In summary, CQMS can be specifically calculated as follows:

$$\begin{aligned} A_{\mathrm{smog},\lambda,t_1} &= -\frac{\log(T_{\lambda,t_1})\cdot V_{t_1}}{l_{t_1}} \\ &= -\frac{\log(T_{\lambda,t_1})\cdot \pi \cdot l_{\mathrm{pixel}} \cdot \sum_{i=a}^{b} [f_{t_1}(x_i)]^2}{2\sqrt{f_{t_1}(x_0)^2 - y_0^2}} \end{aligned} \tag{9}$$

CQMS is theoretically a constant value for the muzzle smoke produced by the same propellant charge at a certain wavelength, and CQMS is proportional to the maximum mass and absorptivity of muzzle smoke. Therefore, CQMS can be used to evaluate the danger level of muzzle smoke produced by different propellant charges, and CQMS is proportional to the danger level of muzzle smoke.

2.2. Minimization of the Impact of the Experimental Errors. Both CQMS and smoke volume are fixed values at t_1. Although the experimental errors of T_{λ,t_1}, V_{t_1}, and l_{t_1} are inevitable, the impact of the experimental errors on CQMS can be minimized, that is, to find values of T_{λ,t_1}, V_{t_1}, and l_{t_1} when the partial derivative of $A_{\mathrm{smog},\lambda,t_1}$ to T_{λ,t_1}, V_{t_1}, and l_{t_1} takes the minimum

$$\begin{aligned} \arg\min\Bigg\{ F(T_{\lambda,t_1}, l_{t_1}) \Bigg| F(T_{\lambda,t_1}, l_{t_1}) &= \frac{\partial A_{\mathrm{smog},\lambda,t_1}}{\partial T_{\lambda,t_1} \partial V_{t_1} \partial l_{t_1}} \\ &= \frac{1}{T_{\lambda,t_1}\cdot l_{t_1}^2 \ln 10},\ l > 0,\ 1 > T_\lambda > 0 \Bigg\} \end{aligned} \tag{10}$$

Eq 4 reveals the functional relationship between l_{t_1} and T_{λ,t_1}

https://doi.org/10.1021/acsomega.2c07764
ACS Omega 2023, 8, 7950−7955

$$l_{t_1} = -\frac{\log(T_{\lambda,t_1})\cdot V_{t_1}}{A_{\mathrm{smog},\lambda,t_1}} \tag{11}$$

Substituting eq 11 into eq 10

$$\arg\min\left\{F(T_{\lambda,t_1})\middle| F(T_{\lambda,t_1}) = \frac{\partial A_{\mathrm{smog},\lambda,t_1}}{\partial T_{\lambda,t_1}\partial V_{t_1}\partial l_{t_1}} = \frac{A^2_{\mathrm{smog},\lambda,t_1}}{T_{\lambda,t_1}(\log(T_{\lambda,t_1}))^2 V^2_{t_1}\ln 10},\ 1 > T_\lambda > 0\right\} \tag{12}$$

Solving eq 12

$$T_{\lambda,t_1} = e^{-2} \cong 13.53\% \tag{13}$$

Therefore, the experimental errors of T_{λ,t_1}, V_{t_1}, and l_{t_1} have the least impact on CQMS when T_{λ,t_1} is 13.53%.

2.3. Experimental Method. Seven firings with the same propellant charge of a 30 mm gun were observed in the field environment to verify the effectivity of CQMS characterizing muzzle smoke. A visible light source and the high-speed camera were placed on both sides of the muzzle, and the gun was preheated before the start timing of the experiment. Parameters of the camera and experimental conditions are shown in Table 1.

Table 1. Parameters of High-Speed Camera and Experimental Conditions

parameter	value
high-speed camera	
camera type	FASTCAM Mini UX50 type 160K-C-16G
camera lens	AF Nikkor 50 mm f/1.8D
record rate (fps)	4000
shutter speed (s)	1/256000
image width	1280
image height	512
experimental conditions	
distance from the camera to muzzle (m)	15
light source location (x_0, y_0) (m)	(1.37, −0.143)

In this experiment, images taken by the high-speed camera were saved in the Bayer format of 16Bit, which not only guaranteed the accuracy of the data but also avoided the demosaic process inside the camera. The pixel where the light source was located belongs to the blue channel, and the corresponding center wavelength was 460 nm. Since the attenuation of the short-distance transmission of visible light in the atmosphere could be ignored, the transmittance T_λ was given by

$$T_\lambda(i) = \frac{I_{\lambda,t=t_i}}{I_{\lambda,t=t_0}} \times 100\%,\ i = 1, 2, 3, \ldots \tag{14}$$

where $I_{\lambda,t=t_i}$ indicates the intensity value of the pixel corresponding to the light source at the moment of t_i.

In order to meet the requirements of the transmittance test, the shutter speed was set to be the shortest, which makes it difficult to see the edges of the muzzle smoke in the saved original images. Therefore, gamma correction was performed on the original images first, then the position of discrete pixels on the edge of the smoke was obtained through image processing, and finally, the smoke volume V and optical path length l were calculated according to eqs 7 and 8.

3. RESULTS AND DISCUSSION

3.1. Experimental Result Analysis. A set of the muzzle smoke images captured by the high-speed camera are shown in Figure 2, the existence time of muzzle smoke could be divided into two stages: muzzle smoke in Stage 1 appeared in the form of a whole cloud, and the edge of the smoke was clear; muzzle smoke in Stage 2 appeared in the form of two separated clouds of smoke, and the edge of the smoke was blurred.

Stage1 started with the moment that the projectile emerged from the barrel (denoted as t_0 = 0 ms), the smoke was then quickly expelled from the inside of the barrel, the mass of the smoke outside the muzzle increased until the smoke inside the barrel was totally discharged. With regard to the propellant charge used in this experiment, in the first half of Stage 1 (about 0−4 ms), besides the smoke, there was also muzzle flash (mainly the prime and intermediate flash with short duration and low intensity, there was no secondary flash). Thus, the absorptivity ε_λ of muzzle smoke with muzzle flash should not be calculated because the absorptivity here is not property of muzzle smoke and the existence of muzzle flash affected the measurement of transmittance T_λ.

On one hand, the blurred edge of Stage 2 indicated that there was a significant mass exchange between the smoke and the surrounding atmosphere. On the other hand, blurred edge of Stage 2 affected the measurement of smoke volume V and optical path length l, and even destroyed the theoretical premise of calculating QMS, for example, the middle section of

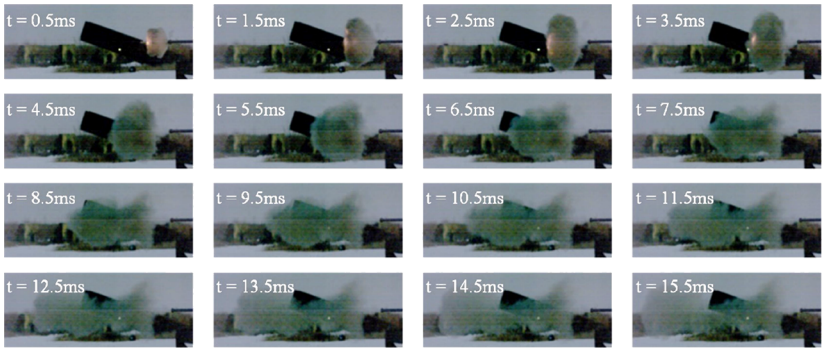

Figure 2. Set of muzzle smoke images captured by a high-speed camera.

https://doi.org/10.1021/acsomega.2c07764
ACS Omega 2023, 8, 7950−7955

the smoke at 14.5 ms in Figure 2 had obviously no axial symmetry. In short, there were some unfavorable factors affecting the actual measurement in the first half of Stage 1 and the second half of Stage 2, therefore, it is better to avoid calculating QMS at these moments.

As shown in Figure 3, after processing a set of high-speed images of muzzle smoke, the curves of transmittance T_λ, smoke

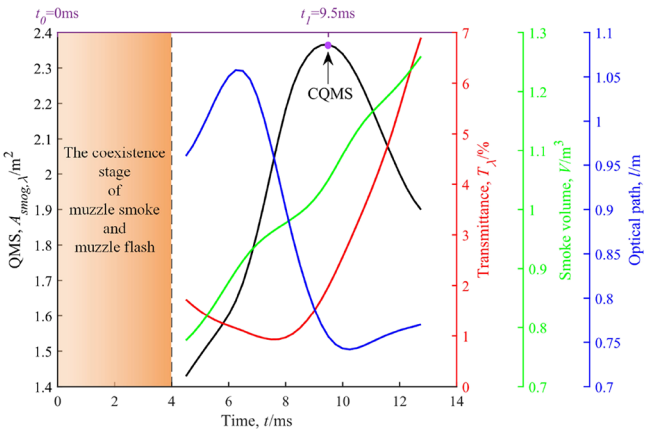

Figure 3. Transmittance, smoke volume, optical path length, and QMS of muzzle smoke in a field experiment.

volume V, and optical path length l with time were obtained, respectively, and then the QMS was calculated. The orange part in Figure 3 represented the stage where muzzle smoke and muzzle flash coexisted, so the time we started to collect data (i.e., 4.5 ms) was slightly later than the end time of the coexistence stage (i.e., 4 ms). The transmittance T_λ decreased slowly in the first stage of muzzle smoke until it reached a minimum value at 7.5 ms, and then rose quickly; the smoke volume V presented an upward trend in both stages; the optical path length l rose first, reached a maximum value at 6.25 ms, then decreased and reached minimum value at 10.25 ms, and then increased slowly. What needs to be reminded is that the smoke volume V has nothing to do with the selected light source position, however, the transmittance T_λ and the optical path length l will vary depending on the position of the light source.

Absorptivity of muzzle smoke could be regarded as a constant value during the time period shown in Figure 3. Considering the mass increase because of the expelled smoke in Stage 1 and the mass decrease because of the mass exchange in Stage 2, it is believed that the change in QMS was due to the change in the mass of muzzle smoke. Since the QMS reaches its maximum value at 9.5 ms, t_1 is 9.5 ms and the corresponding CQMS is 2.37 m^2.

3.2. Measurement Uncertainty Analysis of Experiment Results. The results of the seven sets of experiments at time t_1 are listed in Table 2.

According to "guide to the expression of uncertainty in measurement",[15] for a measurand X is measured directly, consider an input quantity X_i whose value is estimated from n independent observations $X_{i,k}$ of X_i obtained under the same conditions of measurement. In this case, the input estimate x_i is usually the sample mean:

$$x_i = \overline{X}_i = \frac{1}{n}\sum_{k=1}^{n} X_{i,k} \tag{15}$$

Type A evaluation of standard uncertainty $u_A(x_i)$ to be associated with x_i is the estimated standard deviation of the mean:

$$u_A(x_i) = s(\overline{X}_i) = \left(\frac{1}{n(n-1)}\sum_{k=1}^{n}(X_{i,k} - \overline{X}_i)^2\right)^{1/2} \tag{16}$$

As for Type B evaluation, consider an input quantity X_i whose value is estimated from an assumed rectangular probability distribution of lower limit a_- and upper limit a_+. The standard uncertainty $u_B(x_i)$ to be associated with x_i is

$$u_B(x_i) = \frac{a}{\sqrt{3}} \tag{17}$$

where $a = (a_+ - a_-)/2$.

The combined standard uncertainty of a measurement result, suggested symbol $u_c(x_i)$, is

$$u_c(x_i) = \sqrt{u_A(x_i)^2 + u_B(x_i)^2} \tag{18}$$

In this study, transmittance and optical path length were measured directly, and the results based on the combined standard uncertainty are

$$T_{\lambda,t_1} = 1.976 \pm 0.035\ (\%)$$

$$l_{t_1} = 0.758 \pm 0.010\ (\mathrm{m})$$

For a measurand Y is not measured directly, Y is determined from N other quantities X_1, X_2, ⋯, X_N through a functional relationship f:

$$Y = f(X_1, X_2, ..., X_N) \tag{19}$$

An estimate of the measurand or output quantity Y, denoted by y, is obtained from eq 19 using input estimates x_1, x_2, ⋯, x_N for the values of the N input quantities X_1, X_2, ⋯, X_N. Thus, the output estimate y, which is the result of the measurement, is given by

$$y = f(x_1, x_2, ..., x_N) \tag{20}$$

The combined standard uncertainty of the measurement result y, designated by $u_c(y)$ and taken to represent the estimated standard deviation of the result

Table 2. Experiment Results of Seven Sets of Muzzle Smoke with the Same Propellant Charge

	1	2	3	4	5	6	7
T_{λ,t_1} (%)	1.982	1.978	1.897	1.941	1.876	2.160	2.000
V_{t_1} (m^3)	1.1225	1.0503	1.0870	1.0375	1.0323	0.9676	1.0262
l_{t_1} (m)	0.7853	0.7563	0.7479	0.7215	0.7619	0.7987	0.7340

https://doi.org/10.1021/acsomega.2c07764
ACS Omega 2023, 8, 7950−7955

$$u_c(y) = \left(\sum_{i=1}^{N} \left(\frac{\partial f}{\partial x_i} \right)^2 u^2(x_i) + 2 \sum_{i=1}^{N-1} \sum_{j=i+1}^{N} \frac{\partial f}{\partial x_i} \frac{\partial f}{\partial x_j} u(x_i, x_j) \right)^{1/2} \quad (21)$$

In this study, smoke volume and CQMS were not measured directly, and the results based on the law of propagation of uncertainty are

$$V_{t_1} = 1.046 \pm 0.022 \ (\mathrm{m}^3)$$

$$A_{\mathrm{smog},\lambda,t_1} = 2.35 \pm 0.06 \ (\mathrm{m}^2)$$

3.3. Experimental Optimization Discussion. In Section 2.2, it was deduced that the impact of the test errors of T_{λ, t_1}, V_{t_1}, l_{t_1} on $A_{\mathrm{smog}, \lambda}$ can be minimized when the transmittance T_{λ, t_1} is 13.53%. The position of the light source can be changed to meet this condition. Based on the experiment results in Section 3.2, when the optimal transmittance $T_{\lambda, t_1, \mathrm{opt}}$ is 13.53%, the optimal optical path length $l_{t_1, \mathrm{opt}}$ is

$$l_{t_1,\mathrm{opt}} = \frac{-\log_{10} T_{\lambda,t_1,\mathrm{opt}} \cdot V_{t_1}}{A_{\mathrm{smog},\lambda,t_1}} = 0.387 \quad (22)$$

To achieve the optimal optical path length, on the premise that only the y-axis component of the light source position is changed, the y-axis component $y_{0, \mathrm{opt}}$ of the optimal position of the light source is

$$y_{0,\mathrm{opt}} = -\sqrt{y_0^2 + \left(\frac{l_{t_1}}{2} \right)^2 - \left(\frac{l_{t_1,\mathrm{opt}}}{2} \right)^2} = -0.356 \quad (23)$$

Since y_0 is −0.143 m, the light source at the position corresponding to Figure 1 in this experiment should move 0.213 m along the negative direction of y axis.

In addition, it is believed that more accurate results can be obtained using high-speed cameras with higher resolution and fps.

4. CONCLUSIONS

This research provided a quantitative assessment method of muzzle smoke, which is a major source of pollution affecting soldier's health in a field environment. According to the nature of muzzle smoke and the conditions of the field environment, CQMS was defined based on the Beer−Lambert law to characterize the danger level of muzzle smoke, and CQMS was proportional to the danger level of muzzle smoke. Theoretical calculations indicated that when the transmittance is e^{-2}, the impact of the experimental errors on CQMS could be minimized. Seven firings with the same propellant charge of a 30 mm gun were observed in the field environment to verify the effectivity of CQMS. According to the measurement uncertainty analysis performed on the experiment data of seven sets of the same propellant charge, CQMS of the propellant charge used in this experiment is 2.35 ± 0.06 m^2. Because of the difference of mass and absorptivity of muzzle smoke produced by different propellant charges, to a certain extent, CQMS can be regarded as an inherent parameter of the propellant charge.

AUTHOR INFORMATION

Corresponding Authors

Chen-guang Zhu − *School of Chemistry and Chemical Engineering, Nanjing University of Science and Technology, Nanjing 210094, P. R. China*; Email: zhucg@njust.edu.cn

Yan Li − *School of Chemistry and Chemical Engineering, Nanjing University of Science and Technology, Nanjing 210094, P. R. China*; orcid.org/0000-0003-3483-4970; Email: yanli@njust.edu.cn

Authors

Chenguang Yan − *School of Chemistry and Chemical Engineering, Nanjing University of Science and Technology, Nanjing 210094, P. R. China*

Mingxing Zhang − *School of Chemistry and Chemical Engineering, Nanjing University of Science and Technology, Nanjing 210094, P. R. China*

Complete contact information is available at: https://pubs.acs.org/10.1021/acsomega.2c07764

Notes

The authors declare no competing financial interest.

ACKNOWLEDGMENTS

This work was supported by the National Natural Science Foundation of China [Grant number: 51676100] and the Open Project Fund from the National Key Laboratory of Applied Physical Chemistry [Grant number: WDYX22614260204].

REFERENCES

(1) Stuebing, E. W.; Lucia, E. A.; Verderame, F. D.; Pinto, J. J.; Doherty, R. W. *The Nature of Gun Smoke and Dust Obscuration Due to Cannon Firing*; Technical report, 1979.

(2) Nelson, N.; Horvath, S. M.; Eichna, L.; Walpole, R. *Determination of the Characteristics and Effects upon the Crew of Gun Fumes from Firing of the Weapons in the M4A4E1 Tank*; Armored Medical Research Lab, Project No. 3-Toxic Gases in Armored Vehicles Supplemental Report on Sub-Project 3−1, Fort Knox, Kentucky, US, 1943.

(3) Thiboutot, S.; Brochu, S. Assessment and Sustainment of the Environmental Health of Military Live-fire Training Ranges. In *Energetic Materials and Munitions: Life Cycle Management, Environmental Impact and Demilitarization*; Wiley, 2019; pp. 47−74.

(4) Zhou, Z.; Etinger, I. C.; Metze, F.; Hauptmann, A.; Waibel, A. Gun Source and Muzzle Head Detection. *Electron. Imag.* **2020**, *32*, 181-1−187-11.

(5) Carfagno, S. P.; Rudyj, O. N. *Relationship Between Propellant Composition and Flash and Smoke Produced by Combustion Products*; Franklin Inst Philadelphia Pa Labs for Research and Development: Philadelphia, US, 1959.

(6) Brodman, B. W.; Devine, M. P.; Schwartz, S. Propellant charge with reduced muzzle smoke and flash characteristics. U.S. Patent, 4,315,785, 1982.

(7) Brochu, S.; Poulin, I.; Faucher, D.; Diaz, E.; Walsh, M. R. *Environmental Assessment of Small Arms Live Firing: Study of Gaseous and Particulate Residues Environmental Chemistry of Explosives and Propellant Compounds in Soils and Marine Systems: Distributed Source Characterization and Remedial Technologies*; ACS Publications: 2011; Vol. *1069*, pp. 29−47.

(8) Li, S. Y.; Tao, Z. G.; Ding, Y. J.; Liang, H.; Zhao, X. Z.; Xiao, Z. L.; Li, C. Z.; Ou, J. Y. Gradient Denitration Strategy Eliminates Phthalates Associated Potential Hazards During Gun Propellant Production and Application. *Propellants, Explos., Pyrotech.* **2020**, *45*, 1156−1167.

https://doi.org/10.1021/acsomega.2c07764
ACS Omega 2023, 8, 7950−7955

(9) Wang, H.; Sun, M.; Feng, W. Study on the Measurement Technique for Muzzle Smoke and Flash of Deterred Propellants. *Chin. J. Explos. Propellants* **2002**, *25*, 57−58.
(10) Wang, J.; Li, H. A New-style Testing System of Muzzle Smoke Consistency. *J. Detect. Control* **2009**, S1.
(11) Pan, W. J.; Zhou, K. D.; He, L.; Du, E. W.; Li, M. J.; Jiang, J. Research on a Photoelectric Detection System of Muzzle Smoke of Small Arms Based on the Characterization of Light Transmittance. *J. Ordnance Equip. Eng.* **2017**, *159*, 137−140.
(12) Du, E. W.; Jiang, J.; Liu, J. N.; Zou, H. Methods and Research on Detection of Transmittance of Muzzle Smoke. In *14th IEEE International Conference on Electronic Measurement & Instruments (ICEMI)*, 2019; pp. 942−948.
(13) Steward, B. J.; Gross, K. C.; Perram, G. P. Characterization and Discrimination of Large Caliber Gun Blast and Flash Signatures. In *Airborne Intelligence, Surveillance, Reconnaissance (ISR) Systems and Applications IX*; International Society for Optics and Photonics: 2012; vol. *8360*, p. 836006.
(14) Zhao, B. M.; Zhao, H. L.; Yang, L. X.; Li, X.; Chen, X. M.; Zhao, Y.; Zhang, H.; Jin, J. W.; Li, L. D. A Measurement Method for Gun Muzzle Smoke Aggregates of Propellants. *Chin. J. Energ. Mater.* **2013**, *21*, 347−350.
(15) Working Group 1 of the Joint Committee for Guides in Metrology (JCGM/WG 1). *Evaluation of measurement data—Guide to the Expression of Uncertainty in Measurement*, 1st edition; JCGM, 2008.

https://doi.org/10.1021/acsomega.2c07764
ACS Omega 2023, 8, 7950−7955